17 August 1979, Volume 205, Number 4407 SCIENCE

Solid State Electrodes for High Energy Batteries

D. W. Murphy and P. A. Christian

Summary. A new class of electrode materials for high energy density, rechargeable batteries based on topochemical reactions of lithium and transition metal compounds is evolving. The physical and structural properties relevant to the ability of transition metal oxides with framework structures to topochemically incorporate lithium are discussed. Perovskite-related structures are particularly attractive hosts for lithium.

The current interest in the development of more efficient and convenient methods for the utilization of our energy resources has prompted the study of several new types of secondary (rechargeable) batteries in laboratories throughout the world. Some of the applications envisioned for these advanced batteries are vehicle propulsion, off-peak electric energy storage, photovoltaic energy storage, and self-contained power sources for electronic devices. The predominant types of batteries currently under development include the following.

1) Advanced aqueous-based systems such as nickel-zinc, zinc-bromine, and zinc-air.

2) The sodium-sulfur battery.

3) Lithium-metal sulfide batteries with molten salt electrolytes.

4) Ambient-temperature lithium batteries.

These and related systems were reviewed by Cairns and Shimotake (*1*). The ranges of energy and power density expected from these battery systems are summarized in Fig. 1.

The aqueous-based systems are attractive in that they utilize technology closely related to that employed in the fabrication of traditional batteries. Their eventual utilization depends on improvements in the cycle life of the zinc electrode.

The sodium-sulfur battery has a liquid sodium anode and a molten sulfur cathode separated by a solid electrolyte, such as beta alumina, through which only sodium ions diffuse (*2*). This battery must be operated at elevated temperatures (300° to 350°C) in order to keep the electrode materials molten. Another type of high-temperature (400° to 450°C) cell employs a molten salt electrolyte with an alloy of lithium and aluminum as the anode and a metal sulfide (usually FeS or FeS_2) as the cathode (*3*). Both the sodium-sulfur and the lithium-metal sulfide batteries require exotic structural materials to resist the highly corrosive polysulfides and molten salts. The high temperatures required for these batteries will probably restrict their use to the largest and most controlled applications, such as load leveling and perhaps vehicle propulsion.

In this article we limit our discussion to the fourth and newest type of battery system, ambient-temperature lithium batteries. The motivation for using lithium as the anode material lies in the fact that it is the lightest metal and also the most electropositive metal in the electromotive series. In our work, we are concerned primarily with the factors that lead to reversibility at the cathode. Some of the trends observed are presented.

Intercalation

The reaction of lithium and most solid inorganic compounds that might be considered for use as cathode materials is a displacement reaction such as the hypothetical one shown in Eq. 1

$$2MO_2 + 2Li \rightarrow M_2O_3 + Li_2O \qquad (1)$$

where M is a general metal. These displacement reactions, which involve extensive bond breakage, atomic reorganization, and formation of new bonds, are generally not reversible near room temperature. However, one type of reaction that is generally reversible is the intercalation reaction. An ideal intercalation reaction involves the interstitial introduction of a guest species into a host compound without structural modification of the host. Such a reaction is reversible because similar transition states are readily achieved for both the forward and the reverse reactions, leading to close compliance with the thermodynamic principle of microscopic reversibility. In an actual intercalation reaction, the bonding within the host may be slightly perturbed (for instance, a slight expansion of the structure may occur). Similar reactions which depend on the structure of the host but result in somewhat larger structural modifications, such as cleavage of certain bonds, are termed topotactic or topochemical. These reactions may be either reversible or irreversible depending on the specific nature of the structural changes. The terms intercalation, topotactic, and topochemical are, unfortunately, often used interchangeably. Some recognized intercalation reactions include hydrogen dissolution in platinum group metals, bromine complexation by graphite, water absorption by clays, Lewis base incorporation into layered transition metal dichalcogenides, and reduction of graphite or layered transition metal dichalcogenides with alkali metals.

D. W. Murphy is a member of Technical Staff and P. A. Christian is a postdoctoral fellow at Bell Laboratories, Murray Hill, New Jersey 07974.

0036-8075/79/0817-0651$01.50/0

Electrochemical Intercalation Reactions

The inherent reversibility of intercalation suggests its utility as a mechanism for reversible electrode reactions (Eq. 2),

$$A^+ + e^- + MY_n \rightleftarrows AMY_n \qquad (2)$$

where A and Y are a general alkali metal and anion, respectively. Whittingham and Huggins (*4*) used Li_xWO_3 as nonblocking electrodes for measuring the ionic conductivity of lithium beta alumina. Several workers (*5-7*) recognized the possibility of utilizing intercalation reactions at the cathode of a galvanic cell (Eqs. 3 and 4)

$$Li^+ + e^- \rightleftarrows Li \qquad (3)$$

$$xLi^+ + xe^- + MY_n \rightleftarrows Li_xMY_n \qquad (4)$$

Whittingham (*8*) has shown that the discharge mechanism of several cathodes containing transition metal oxides (for example, V_2O_5 and MoO_3) and sulfides (TiS_2) in nonaqueous lithium cells do indeed involve topochemical incorporation of lithium into the compounds. Extensive studies (*9-12*) have demonstrated that high power densities as well as high energy densities may be obtained for batteries utilizing layered dichalcogenide cathodes.

A number of authors (*5, 6, 13, 14*) have proposed the following basic requirements for solid state cathode materials.

1) Large free energy of reaction, ΔG (affording a high cell voltage).

2) Wide compositional range; that is, x in Eq. 4 (resulting in high cell capacities).

3) High diffusivity of the guest species in the host (allowing high power densities).

4) Minimal structural change as a function of composition (resulting in a reversible reaction).

Additional desirable properties are:

1) Good electronic conductivity (to minimize resistive heat generation and eliminate the need for a conductive additive in the electrode).

2) Low solubility in the electrolyte (to prevent self-discharge).

Van der Waals Bonded Structures

The reactions of compounds with two-dimensional van der Waals bonded structures such as graphite, the early transition metal dichalcogenides, molybdenum trioxide, and transition metal phosphotrichalcogenides with electropositive metals (especially lithium) have been extensively studied. Graphite has a small free energy of reaction with lithium, which renders it unsuitable as a cathode, but many of the other layered compounds have sufficiently high free energies of reaction. The van der Waals gap between the layers of these compounds provides sufficient vacant sites to allow a wide composition range of intercalated lithium (up to approximately one lithium per metal ion) and also a pathway for facile lithium diffusion. Diffusion coefficients of 10^{-8} to 10^{-9} square centimeters per second have been measured for lithium in TiS_2 (*15, 16*). True intercalation occurs in the system Li_xTiS_2 $(0 < x \leq 1)$, whereas most of the other well-characterized layered compounds exhibit some structural changes of the host or phase disproportionation for some lithium stoichiometries. Structural distortions in layered VS_2 (*17*) have been associated with its limited capacity in electrochemical cells. However, substitution of other metal ions for some of the vanadium suppresses these structural distortions and allows the capacity to approach the expected value, which corresponds to one lithium per VS_2. The one-dimensional van der Waals bonded metal trichalcogenides (*8, 18, 19*) and niobium tetraselenide (*20*) also react topochemically with lithium in electrochemical cells.

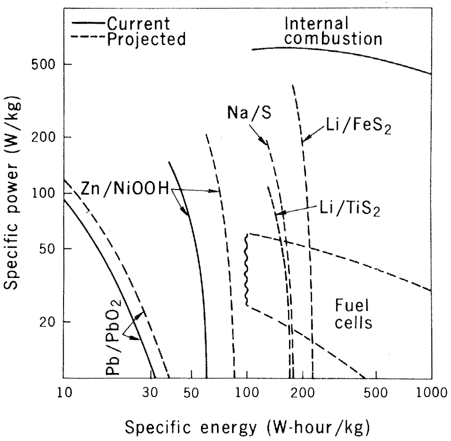

Fig. 1. Specific power and energy from some present-day energy sources and projections for the future based on (*1*).

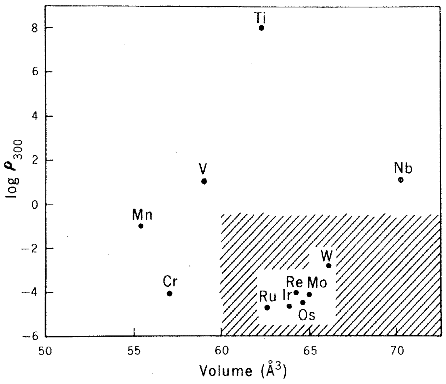

Fig. 2. Resistivity versus unit cell volume for rutile-related MO_2 compounds. Those with values in the shaded region readily incorporate lithium.

The reader is referred to several reviews of intercalation reactions and electrochemistry of van der Waals compounds for a more detailed discussion (*13, 21-24*).

Three-Dimensional Structures

Several factors have prompted us to study the feasibility of using three-dimensionally bonded host lattices (framework structures) as cathode materials rather than van der Waals compounds. One of these factors is the possibility of using electrolyte solvents that are incompatible with van der Waals compounds because these solvents form intercalation compounds, either alone or coordinated to lithium. The high ionic conductivities of several solid electrolytes with framework structures (*25, 26*) suggest that related materials be considered as hosts for lithium incorporation. Finally, compounds with framework structures constitute a considerably larger class of materials than do van der Waals compounds.

Several examples of topochemical lithium incorporation into framework compounds have been reported. Besenhard and Schöllhorn (*27*) have reported topochemical reactions of several chromium oxides. Steele (*28*) has observed lithium incorporation by bornite (Cu_3FeS_4) after electrochemical removal of copper. Lithium intercalation has been proposed as the discharge mechanism of primary lithium cells containing molybdenum oxides with shear structures as cathodes (*29*).

In order to assess the influence of various physical properties on the topochemical incorporation of lithium by three-dimensional framework transition metal oxides, we initially investigated rutile-related transition metal dioxides (*30*). The presence of vacant channels in the rutile structure affords potential sites for lithium, as previously noted (*5, 31*). This large class of compounds provides for a wide variation of potentially important properties such as channel size, electronic conductivity, and structural distortions. Our results suggest that topochemical incorporation of substantial amounts of lithium by these compounds occurs readily provided the channels are sufficiently large and the host structure has metallic conductivity (Fig. 2). Extended lithium ion diffusion in these compounds is contrary to the tenet that macroscopic diffusion in one-dimensional channels will inevitably be blocked by lattice defects. It is also important to note that the cross sections of the channels in these compounds are significantly smaller than the minimum bottleneck proposed by Hong (*26*) for fast lithium ion diffusion in solid electrolytes. Thus, the extent of lithium incorporation is greater in metallic rutiles, perhaps because of more effective screening of Coulombic repulsion between lithium ions. Although metallic conductivity facilitates lithium incorporation in rutiles, substantial lithium incorporation does occur with many compounds having poor electronic conductivity, such as anatase TiO_2 (*32*) and γ-MnO_2 (*33*), which are 10 and 16 percent less dense than their rutile polymorphs.

Model Reactions

Several reactions may be used to mimic the discharge (intercalation) and charge (deintercalation) reactions of the cathode in secondary lithium cells. These reactions have proved to be of great value in screening potential cathode materials since they are rapid and free from the element of art inherent in the fabrication of electrodes. In addition, these reactions have allowed the preparation of pure phases (many previously unknown) present at various states of charge in electrochemical cells. Studies of physical properties of these phases such as crystal structure, conductivity, thermodynamics, magnetic susceptibility, and nuclear magnetic resonance can yield valuable insight into the microscopic nature of the cell reaction and may suggest modifications of the materials to improve cell performance.

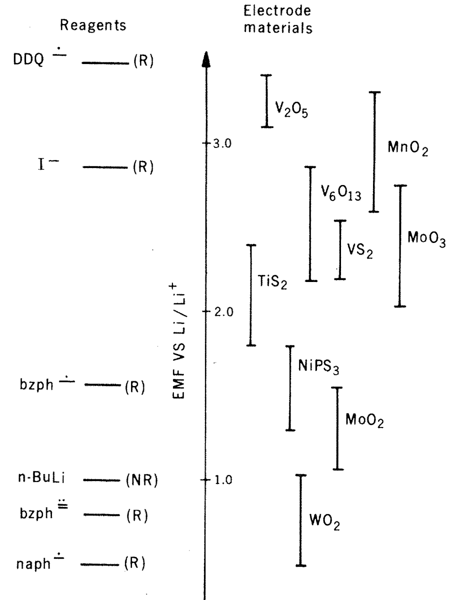

Fig. 3. Potentials of a variety of electrode materials and reagents for modeling cell reactions relative to Li/Li^+. The reduced form of the reagent is shown; (*R*) denotes reversible and (*NR*) denotes irreversible reagents. Other abbreviations: *DDQ*, 2,3-dichloro-4,5-dicyanobenzoquinone; *bzph*, benzophenone; and *naph*, naphthalene. The potentials of the reagents may vary slightly with solvent, concentration, and supporting electrolyte.

Cell discharge involves addition of lithium ions and electrons to the host (Eq. 4). Although the direct reaction of lithium with the host compound has been used to prepare some lithium intercalation compounds (*34, 35*), it more often results in undesirable side reactions. There are several alternative methods for preparing lithium intercalation compounds using milder conditions. Lithium metal dissolved in liquid ammonia is an improved reagent for many intercalation reactions (*36*). Lithium salts of radical anions such as naphthalide may also be used. The easiest and cleanest reagent for many lithium intercalation reactions and for the screening of possible cathode materials is *n*-butyllithium (*n*-BuLi) in hexane (*7, 37, 38*).

The charging half-cell reaction corresponds to reoxidation of the reduced host (Eq. 4 proceeding to the left). Oxidizing agents stronger than the host material are capable of oxidizing the lithium intercalation compound, resulting in the removal of lithium ions and electrons from the structure. Many reagents are sufficiently oxidizing to accomplish this, but some also cause undesirable side reactions, such as the hydrolysis of chalcogenides by aqueous reagents. Both the oxidized and reduced forms of the reagent should be soluble in a nonreactive solvent. A particularly useful reagent is iodine in acetonitrile, which allowed the first preparation of the layered VS_2 from $LiVS_2$ (*17*).

The ideal reagents to model Eq. 4 are themselves reversible oxidation-reduction couples. This reversibility allows a couple to reduce some materials and to oxidize others. For example, iodine oxidizes $LiVS_2$ to VS_2, but lithium iodide reduces V_2O_5 to LiV_2O_5 (*39, 40*). Approximate potentials of selected redox couples and cathode materials are shown in Fig. 3. By a judicious choice of reagent, undesirable side reactions can be avoided. For example, the reaction of V_2O_5 and LiI proceeds cleanly to give LiV_2O_5, whereas additional irreversible reduction occurs with the stronger reducing agent *n*-BuLi.

Solutions of organic radical anions generated by the lithium reduction of naphthalene (naph), benzophenone (bzph), and 2,3-dichloro-4,5-dicyanobenzoquinone (DDQ) are intensely colored. Since these couples span a range of reduction potentials they can be used as indicators to estimate the potential of lithium compounds. If a compound $LiMY_n$ reduces naph to the green naph, its potential versus Li/Li^+ is less than 0.5 volt. Reduction of bzph to the purple bzph indicates a voltage below 1 V, whereas formation of the blue bzph$^{\dot{-}}$ indicates a voltage between ~1.5 and 1.0 V. For example, bzph is unaffected by $LiTiS_2$, reduced to the blue bzph$^{\dot{-}}$ by $LiMoO_2$, and to the purple bzph$^{\ddot{=}}$ by $LiWO_2$. Reduction of iodine to the colorless iodide indicates a voltage below 2.85 V. The red DDQ$^{\dot{-}}$ can be generated by all $LiMY_n$ with reversible potentials less than 3.5 V versus Li/Li^+. Both iodine and DDQ are reduced by $LiTiS_2$, $LiVS_2$, and $LiMoO_3$. Other radical anions, including those of substituted bzph and naph compounds, could provide reagents (or indicators) at virtually any electromotive force between 0 and 3.5 V versus Li/Li^+. The bzph and naph reagents are typically used in tetrahydrofuran, while acetonitrile is preferred for the more oxidizing iodine and DDQ.

Perovskite-Based Structures

Perovskite-type structures characteristically contain cuboctahedron cavities, which are often occupied by large cations such as Ca^{2+}, Ba^{2+}, and less frequently Na^+ or Li^+. This cavity (Fig. 4a) is vacant in a number of compounds typified by ReO_3 (*41*). Similar cavities with one or more of the square faces capped

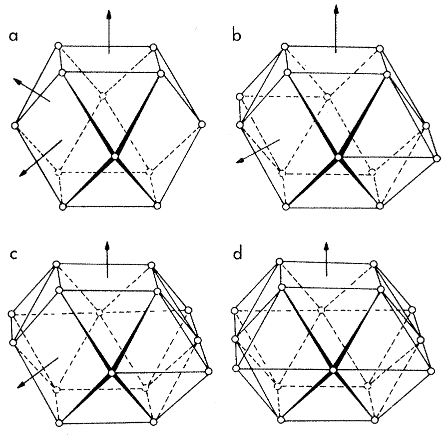

Fig. 4. Perovskite-like cavity of (a) ReO_3, (b) V_2O_5, (c) V_6O_{13}, and (d) $VO_2(B)$. Circles represent oxygen ions. Arrows indicate the direction of channels in the lattice for diffusion of lithium ions.

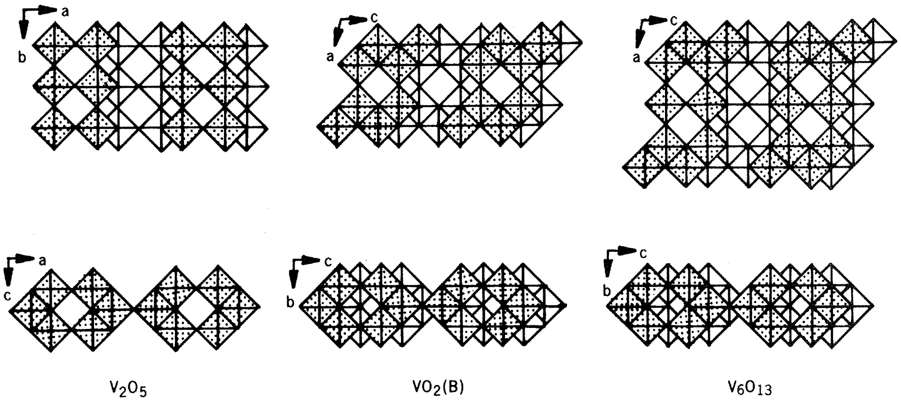

Fig. 5. Corresponding views of V_2O_5, V_6O_{13}, and $VO_2(B)$ constructed from idealized MO_6 octahedra.

by an additional anion are found in shear structures derived from the ReO_3 structure. Idealized representations of the cavities present in some vanadium oxide shear structures are shown in Fig. 4, b to d. All of these compounds contain an extended network of cavities generated by the sharing of equivalent square faces of the individual cavities. Assuming that lithium can diffuse between cavities only by passing through the square faces (Fig. 4), the potential dimensionality for lithium diffusion through the structure is reduced by capping of these faces. The small value for lithium ion diffusivity of Li_xWO_3 suggests that in this case considerations other than the size of the bottleneck may predominate. The results of a neutron diffraction study of $Li_{0.36}WO_3$ (*42*) were too ambiguous to allow assignment of the lithium ion positions precisely, but it was inferred that the lithium ions were most likely centered in puckered cavities, each coordinated by four coplanar oxygens. However, this type of coordination for lithium is unprecedented. The same apparent position could also result from a disordering of lithium among 12 equivalent distorted square pyramidal sites within the idealized cavity, or as the average position of lithium rapidly hopping among these sites. Lithium ions occupy such distorted square pyramidal sites in the bronze $Li_{0.3}V_2O_5$ (*43*).

Lithiation of the metallic compound ReO_3 with *n*-BuLi affords $Li_{2.3}ReO_3$, in which the cubic symmetry of ReO_3 (unit cell axis a = 3.751 Å) is reduced to orthorhombic (unit cell axes a = 5.618 Å, b = 4.984 Å, c = 3.730 Å), presumably resulting in an elongation of the cuboctahedral cavity in one direction and a contraction in another. This makes the faces of the cavity inequivalent and may also affect the dimensionality of lithium diffusion. Although $Li_{2.3}ReO_3$ is readily reconverted to ReO_3 by oxidation with I_2, the corresponding electrochemical lithiation and delithiation reactions are sluggish. The presence of more than one lithium per cavity (Fig. 4a) necessitates occupation of sites other than that in the center of the cavity.

An idealized V_2O_5 structure may be derived from the ReO_3 structure by removing oxygens from every second (200) plane and closing the structure along the shear vector ½[101]. The resulting shear structure (*44, 45*) (Fig. 5) consists of distorted VO_6 octahedra joined by edge sharing among themselves along [001] into single zigzag chains linked together by corner sharing to form single sheets. The sheets are joined by means of additional corner sharing into a three-dimensional structure. Alternatively, the coordination of vanadium may be viewed as square pyramidal with the corner-shared V-O bonds along [010] forming asymmetric V=O---V units (*46, 47*). Although the actual structure of V_2O_5 is highly distorted, it may be viewed as containing bicapped perovskite-like cavities with two opposite square faces capped with oxygens (Fig. 4b). This capping restricts the potential lithium motion to the (100) plane. Also, capping produces two additional square pyramidal sites with the capping oxygens at the apexes. As in $Li_{2.3}ReO_3$, the cavity in LiV_2O_5 is elongated compared to that in V_2O_5. In LiV_2O_5 the number of lithium ions equals the number of cavities. Intercalation of lithium into V_2O_5 has been viewed as involving the separation of weakly bonded two-dimensional layers (*8*) analogous to the metal dichalcogenides. The failure of V_2O_5 to incorporate the larger cations Na^+ and Me_4N^+ under mild conditions suggests that V_2O_5 is more appropriately viewed as a framework host rather than a van der Waals host (*40*).

The V_6O_{13} structure may be regarded as a shear structure of V_2O_5 (*44, 45, 48*). The V_6O_{13} structure (Fig. 5) contains distorted VO_6 octahedra joined by extensive edge sharing into both single and double zigzag chains running parallel to [010]. Both the single and double chains are linked by additional edge sharing into single and double sheets, respectively, both lying parallel to the (100) plane. The sheets are interleaved and joined together by corner sharing to form the three-dimensional framework. This structure contains tricapped perovskite-like cavities (Fig. 4c) joined through shared square faces. The three open faces of the cavity should permit lithium ion diffusion along [010] with the possibility for exchange between pairs of adjacent channels. There are two cavities and 30 square pyramidal sites (not all equivalent) per V_6O_{13} formula unit. The maximum lithium stoichiometry attainable with *n*-BuLi is $Li_8V_6O_{13}$ (*49*). Lithium incorporation results in elongation of the unit cell in the direction of the channels. Virtually all of the incorporated lithium may be removed from $Li_8V_6O_{13}$ by treatment with DDQ.

Another vanadium oxide, the metastable $VO_2(B)$, is thought to have a structure related to those of V_2O_5 and V_6O_{13} (*44, 50–52*). The structure proposed for $VO_2(B)$ (Fig. 5) may be visualized simply as that obtained by removing the sheets of single chains from the V_6O_{13} structure described above. The resulting structure is closely related to that of $Na_{0.2}TiO_2$ described by Andersson and Wadsley (*53*). Such a structure can also be derived from the ReO_3-type lattice by a double shear (*44*). The $VO_2(B)$ lattice contains perovskite cavities with four faces capped (Fig. 4d), leaving only the possibility of uniaxial lithium diffusion parallel to [010].

Although ReO_3, V_2O_5, V_6O_{13}, and $VO_2(B)$ readily incorporate lithium topochemically at room temperature, none incorporate sodium or larger cations at significant rates. This is especially significant for V_2O_5, and leads to the conclusion that weak vanadium oxygen bonding between layers persists in LiV_2O_5.

Lithium incorporation by each of the above compounds results in a predominantly uniaxial expansion of the perovskite-like cavity. The strength of the bonding in the direction of expansion appears to be a major factor in determining the extent of lithium incorporation before the catastrophic rupture of M-O bonds. Linear, asymmetric V=O---V linkages are the only bonds present in V_2O_5 in the direction of elongation. The longer V---O bonds are easily ruptured, allowing mica-like cleavage of V_2O_5

crystals parallel to (010). Some elongation of this linkage on formation of LiV_2O_5 is tolerated, but further reduction below 2.5 V undoubtedly leads to additional stretching and eventual cleavage of the V---O bonds followed by a major structural reorganization. Both V_6O_{13} and VO_2(B) are completely edge-shared in the direction of expansion, thus increasing their resistance to bond cleavage. The reversible reduction of V_2O_5 corresponds to the incorporation of one lithium per cavity. However, eight lithium ions can be reversibly incorporated per V_6O_{13} formula unit, corresponding to four lithiums per cavity. Similarly, VO_2(B) reversibly incorporates about 3.5 lithiums per cavity.

Electrochemical Cells

Use of V_2O_5 as a cathode material in nonaqueous lithium secondary batteries was originally reported by Walk and Gore (*54*). However, there are some significant limitations to the use of V_2O_5, including low electronic conductivity, the oxidation of organic electrolyte solvents at the high voltages necessary for charging, the finite solubility of V_2O_5 in organic solvents, and the irreversible reduction of V_2O_5 at potentials only slightly below that for the reversible reaction.

The use of the metallic compound V_6O_{13} as the active cathode material (*49*) results in lower cell voltages (2.8 to 2.2 V) than for V_2O_5 cells (3.3 to 3.0 V), thus minimizing electrolyte oxidation. In addition, V_6O_{13} is virtually insoluble in organic solvents. The most significant improvement is that irreversible reduction with lithium does not occur above 1 V (that is, with *n*-BuLi), and cells with a lithium anode and a lithium hexafluoroarsenate in propylene carbonate electrolyte ($Li/LiAsF_6$, PC/V_6O_{13}) may be temporarily short-circuited without irreversible reduction. There are several distinct breaks in cell voltage as a function of the state of charge as well as subtle differences between discharge and charge, suggesting complexities in the $Li-V_6O_{13}$ phase diagram. Small test cells with V_6O_{13} cathodes maintain their voltage characteristics and capacities with cycling better than those made with any other cathode material we have studied. Typical behavior is illustrated by the voltage curves in Figs. 6 and 7. Based on a limiting stoichiometry of $Li_8V_6O_{13}$ and an average cell voltage of 2.2 V, the theoretical energy density of the Li/V_6O_{13} system can be estimated as 800 watt-hours per kilogram.

The results of several experiments suggest that lithium ion diffusivity decreases with increasing lithium ion content in V_6O_{13}. For 10- to 50-micrometer particles, the extent of lithiation by *n*-BuLi and in electrochemical cells (Fig. 6) corresponds to approximately $Li_4V_6O_{13}$. With 1- to 5-μm particles under similar conditions, treatment with *n*-BuLi affords $Li_8V_6O_{13}$ whereas electrochemical cells exhibit capacities corresponding to $Li_6V_6O_{13}$. The additional capacity provided by the use of the smaller particles of V_6O_{13} results in a plateau at ~2.2 V. The capacity of this plateau decreases when the cell is operated below 20°C (Fig. 7). Conversely, additional capacity is obtained at 2.2 V for cells having the larger particles of V_6O_{13} by heating them to 80°C. To obtain the maximum capacity from V_6O_{13} cells an electronically conductive material must be added to the cathode, since highly lithiated V_6O_{13} is a poor electronic conductor. As is the case for rutile-related oxides, a reduction in lithium ion mobility may result from a decrease in electronic conductivity.

Although VO_2(B) is structurally very similar to V_6O_{13}, $Li/LiAsF_6$,PC/VO_2(B) cells exhibit lower voltages (2.8 to 1.5 V), lower capacity, and poorer rechargeability than those with V_6O_{13}. Treatment of VO_2(B) with *n*-BuLi results in the incorporation of approximately 2/3 lithium per VO_2(B) formula unit, whereas less than 1/2 lithium per VO_2(B) can be cycled in the electrochemical cells.

Future Prospects

Although the deliberate search for topochemical electrode materials was initiated only recently, several classes of promising compounds have already been identified. The rate at which new electrode materials are being reported suggests that even more promising materials will follow. An empirical understanding of the factors influencing the lithium incorporation process is evolving concurrently with the identification of these new electrode materials. The use of model reactions and simple test cells allows easy screening of potential electrode materials. The only electrode material utilizing lithium intercalation for which serious engineering projections for large-scale applications have been made is TiS_2 (*11, 12*). However, on the basis of results obtained with small laboratory test cells, several other new elec-

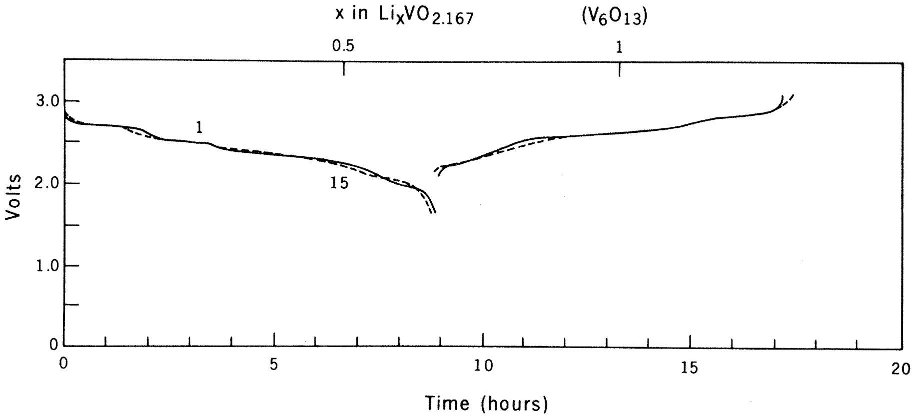

Fig. 6. Cycle data from a cell containing 8.5 milligrams of 10- to 50-μm V_6O_{13}. The electrolyte was $LiAsF_6$ in propylene carbonate. The current was 0.2 milliampere. Cycle numbers are indicated.

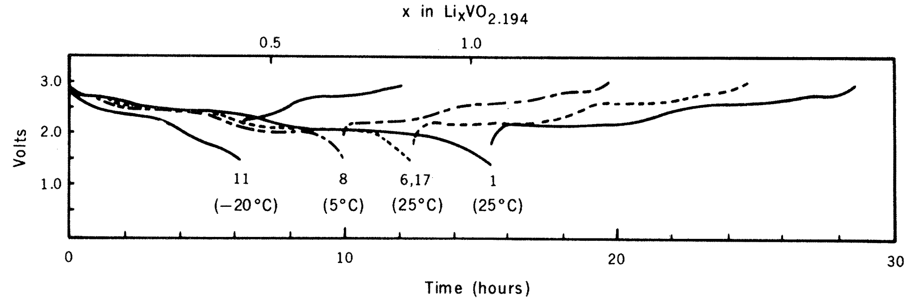

Fig. 7. Cycle data for a cell containing 19.4 milligrams of 1- to 5-μm V_6O_{13}. The current was 0.2 milliampere. The capacity decreases at lower temperatures and recovers when the cell is returned to room temperature. Cycle numbers are indicated.

trode materials appear to be promising candidates as well, most notably V_6O_{13} and $NbSe_3$ (*55*).

Although we have restricted this discussion to cathode materials, more than a good cathode material is required to make a practical battery. The lithium electrode, which functions by a metal stripping and plating mechanism, presents a cycle life problem because of poor stripping efficiency. Improvements in lithium plating efficiency have been achieved through the use of lithium-aluminum alloy as the source of lithium (*56*), electrolyte solvents such as dioxolane (*12*) or 2-methyltetrahydrofuran (*57*), and solutes such as lithium hexafluoroarsenate or lithium tetraorganoborates (*58, 59*). There are also a myriad of other considerations, such as safety and the effects of overcharging or cell reversal, which must be evaluated in a development program before the full potential of these new, high energy battery systems can be assessed.

References and Notes

1. E. J. Cairns and H. Shimotake, *Science* **164**, 1347 (1969).
2. N. Weber and J. T. Kummer, in *Advances in Energy Conversion Engineering* (American Society of Mechanical Engineers, New York, 1967), p. 913; G. C. Farrington and J. L. Briant, *Science* **204**, 1371 (1979).
3. D. R. Vissers, Z. Tomczuk, R. K. Steunenberg, *J. Electrochem. Soc.* **121**, 665 (1974).
4. M. S. Whittingham and R. A. Huggins, in *Fast Ion Transport in Solids*, W. van Gool, Ed. (North-Holland, Amsterdam, 1973), pp. 645-652.
5. B. C. H. Steele, in *ibid.*, pp. 103-122.
6. L. Heyne, in *ibid.*, pp. 123-139.
7. M. B. Armand, in *ibid.*, pp. 665-673.
8. M. S. Whittingham, *J. Electrochem. Soc.* **123**, 315 (1976).
9. J. Broadhead, in *Power Sources 4*, D. H. Collins, Ed. (Oriel, London, 1973), pp. 469-481.
10. M. S. Whittingham, *Science* **192**, 1126 (1976).
11. L. H. Gaines, R. W. Francis, G. H. Newman, B. M. L. Rao, paper presented at the 11th Intersociety Energy Conversion Engineering Conference, Lake Tahoe, September 1976.
12. B. M. L. Rao, G. H. Newman, R. W. Francis, L. H. Gaines, paper presented at the Electrochemical Society Meeting, Atlanta, October 1977.
13. M. S. Whittingham, *Prog. Solid State Chem.* **12**, 1 (1978).
14. W. L. Worrell and A. S. Nagelberg, in *Proceedings of the Symposium and Workshop on Advanced Battery Research and Design* (National Technical Information Service, Springfield, Va., 1976), pp. B2-B12.
15. D. A. Winn, J. M. Shemilt, B. C. H. Steele, *Mater. Res. Bull.* **11**, 559 (1976).
16. M. S. Whittingham and B. G. Silbernagel, in *Solid Electrolytes*, W. van Gool and P. Hagenmuller, Eds. (Academic Press, New York, 1977), pp. 93-108.
17. D. W. Murphy, J. N. Carides, F. J. DiSalvo, C. Cros, J. V. Waszczak, *Mater. Res. Bull.* **12**, 825 (1977).
18. D. W. Murphy and F. A. Trumbore, *J. Electrochem. Soc.* **123**, 960 (1976).
19. R. R. Chianelli and M. B. Dines, *Inorg. Chem.* **14**, 2417 (1975).
20. D. W. Murphy, F. A. Trumbore, J. N. Carides, *J. Electrochem. Soc.* **124**, 325 (1977).
21. D. W. Murphy and F. A. Trumbore, *J. Cryst. Growth* **39**, 185 (1977).
22. F. R. Gamble and T. H. Geballe, in *Treatise on Solid State Chemistry*, N. B. Hannay, Ed. (Plenum, New York, 1976), vol. 3, p. 125.
23. G. L. Holleck and J. R. Driscoll, *Electrochim. Acta* **22**, 647 (1977).
24. J. O. Besenhard and R. Schöllhorn, *J. Power Sources* **1**, 267 (1976).
25. J. B. Goodenough, H. Y-P. Hong, J. A. Kafalas, *Mater. Res. Bull.* **11**, 203 (1976).
26. H. Y-P. Hong, paper presented at the American Chemical Society Meeting, Miami Beach, Fla., September 1978.
27. J. O. Besenhard and R. Schöllhorn, *J. Electrochem. Soc.* **124**, 968 (1977).
28. B. C. H. Steele, in *Superionic Conductors*, G. D. Mahan and W. L. Roth, Eds. (Plenum, New York, 1976), pp. 47-64.
29. B. DiPietro, V. Filippeschi, M. Lazzari, G. Pistoia, B. Scrosati, in *Power Sources 6*, D. H. Collins, Ed. (Academic Press, New York, 1977), pp. 527-536.
30. D. W. Murphy, F. J. DiSalvo, J. N. Carides, J. V. Waszczak, *Mater. Res. Bull.* **13**, 1395 (1978).
31. O. W. Johnson, *Phys. Rev. A* **136**, 284 (1964).
32. M. S. Whittingham and M. B. Dines, *J. Electrochem. Soc.* **124**, 1387 (1977).
33. H. Ikeda, T. Saito, H. Tamura, *Manganese Dioxide Symp. Proc.* **1**, 384 (1975).
34. W. P. F. A. M. Omloo and F. Jeilinek, *J. Less-Common Met.* **20**, 121 (1970).
35. D. Guérard and A. Hérold, *Carbon* **13**, 337 (1975).
36. M. Danot, A. Leblanc, J. Rouxel, *Bull. Soc. Chim. Fr.* (1969), p. 2670.
37. M. B. Dines, *Mater. Res. Bull.* **10**, 287 (1975).
38. D. W. Murphy, F. J. DiSalvo, G. W. Hull, J. V. Waszczak, *Inorg. Chem.* **15**, 17 (1976).
39. D. W. Murphy, P. A. Christian, J. W. Carides, F. J. DiSalvo, paper presented at the International Conference on Fast Ion Transport in Solids, Lake Geneva, Wis., 21 to 25 May 1979.
40. D. W. Murphy, P. A. Christian, F. J. DiSalvo, J. V. Waszczak, *Inorg. Chem.*, in press.
41. G. M. Clark, *The Structures of Non-Molecular Solids* (Wiley, New York, 1972), pp. 148-150.
42. P. J. Wiseman and P. G. Dickens, *J. Solid State Chem.* **17**, 91 (1976).
43. A. Hardy, J. Galy, A. Casalot, M. Pouchard, *Bull. Soc. Chim. Fr.* (1965), p. 1056.
44. K. Kawashima, K. Kosuge, S. Kachi, *Chem. Lett.* (1975), p. 1131.
45. K-A. Wilhelmi, K. Waltersson, L. Kihlborg, *Acta Chem. Scand.* **25**, 2675 (1971).
46. H. G. Bachmann, F. R. Ahmed, W. H. Barnes, *A. Kristallogr.* **115**, 110 (1961).
47. A. Bystöom, K-A. Wilhelmi, O. Brotzen, *Acta Chem. Scand.* **4**, 1119 (1950).
48. J. S. Anderson and B. G. Hyde, *J. Phys. Chem. Solids* **28**, 1393 (1967).
49. D. W. Murphy, P. A. Christian, F. J. DiSalvo, J. N. Carides, *J. Electrochem. Soc.* **126**, 497 (1979).
50. F. Théobald, R. Cabala, J. Bernard, *J. Solid State Chem.* **17**, 431 (1976).
51. F. Théobald and J. Bernard, *C. R. Acad. Sci. Ser. C* **268**, 60 (1969).
52. T. Sata and Y. Ito, *Bull. Tokyo Inst. Technol.* **98**, 1 (1970).
53. S. Andersson and A. D. Wadsley, *Acta Crystallogr.* **15**, 201 (1962).
54. C. R. Walk and J. S. Gore, paper presented at the Electrochemical Society Meeting, Toronto, 11 to 16 May 1975.
55. J. Broadhead and F. A. Trumbore, paper presented at the Electrochemical Society Meeting, Chicago, 13 to 18 May 1973.
56. B. M. L. Rao, R. W. Francis, H. A. Christopher, *J. Electrochem. Soc.* **124**, 1490 (1977).
57. V. Koch, U.S. Patent 4,118,550 (1978).
58. L. P. Klemann and G. H. Newman, U.S. Patent 4,060,674 (1977).
59. T. A. Whitney and L. P. Klemann, U.S. Patent 4,104,450 (1978).

60. We gratefully acknowledge the valuable contributions of our colleagues J. N. Carides, F. J. DiSalvo, and F. A. Trumbore, who are an integral part of this research program. We are indebted also to J. Broadhead and J. H. Wernick for helpful discussions and critical reviews of the manuscript.

Effects of Energy Conservation in Residential and Commercial Buildings

Eric Hirst and Bruce Hannon

In this article, we evaluate the economic and the net (direct and indirect) energy and employment effects of adopting different conservation programs and new technologies in residential and commercial buildings. The time span considered is from now to the end of the century. Our analyses were conducted with detailed engineering-economic models developed at Oak Ridge National Laboratory for each of the two building sectors (*1*) and input-output models developed at the University of Illinois (*2*).

The scenarios include the following:

1) The first scenario is a base line in which fuel prices rise over time as predicted by Department of Energy (DOE) and Brookhaven National Laboratory (BNL) energy models. Population, households, commercial floor space, and per capita income all grow at rates roughly comparable to their historical values.

2) The National Energy Plan (NEP) is a conservation case that includes higher gas and oil prices plus regulatory, financial incentive, and information programs authorized by the 94th Congress and expanded upon in the April 1977 NEP.

3) The third scenario is a conservation case that differs from the preceding one

---

Dr. Hirst is on the staff of the Energy Division, Oak Ridge National Laboratory, Oak Ridge, Tennessee 37830. Dr. Hannon is a member of the Energy Research Group, Office of the Vice-Chancellor for Research, University of Illinois, Urbana 61801.

0036-8075/79/0817-0656$01.50/0